Fluid-deposited fracture-margin ridges in Margaritifer Terra, Mars

Rebecca J. Thomas[1], Sally Potter-McIntyre[2] & Brian M. Hynek[1,3]

[1] LASP, University of Colorado, Boulder, CO 80309, USA, [2] Southern Illinois University, Geology Department, Parkinson Lab Mailcode 4324, Carbondale, IL 62901, [3] Department of Geological Sciences, University of Colorado, 399 UCB, Boulder, CO 80309, USA. rebecca.thomas@lasp.colorado.edu

1. Introduction: Astrobiological potential of fracture-margin mineralization

Sites where mineral deposition occurred in association with fluid flow from the subsurface are excellent targets as which to seek evidence for past life on Mars because:

1. aqueous environments are favorable to life, and
2. precipitated minerals can encase biosignatures, protecting them from degradation in the oxidizing environment at the Martian surface [1,2].

We report **ridges at the margins of broad fractures in Margaritifer Terra**, and conduct morphological and stratigraphic analysis of two key sites to determine their probable mode of formation. On the basis of this analysis and through analogy with similar structures on Earth, we conclude that the two ridge types are best explained by **low-temperature mineralization in the subsurface** and **surface deposition from a hydrothermal system**, respectively, both of which **have the potential to preserve astrobiological evidence**.

Fig. 1. Mineral precipitation (white/red) and microbial mats (green) at a site of fluid upwelling on Earth (Big Bubbling Spring, Utah).

2. Approach to Analysis

Using Mars Reconnaissance Orbiter (MRO) CTX [3], HiRISE [4] and Mars Global Surveyor MOC [5] images, we identified 12 candidate sites of fracture-margin mineralization in Margaritifer Terra, a Noachian highland region just south of the global dichotomy boundary that is extensively cross-cut by Late Hesperian-Amazonian chaos (Ht, Fig. 2) and associated fractures and hosts many floor-fractured impact craters [6,7]. In all but one case, ridges occur at crater floor fractures, indicating that this is a characteristic setting for them.

For the best-imaged examples of two morphologically-distinct ridge types, we:

- Created morphostratigraphic maps using image and thermal inertia [8] data.
- Investigated topography with gridded Mars Laser Altimeter (MOLA) data [9], Mars Express HRSC DTMs [10], and CTX DTMs derived from stereo images using Ames Stereo Pipeline software [11].
- Explored spectral variation in THEMIS decorrelation stretch images (DCS875) [12].
- Investigated relative and absolute surface ages through crater-counting using standard techniques and plots against isochons derived from the Ivanov [13] crater production and Hartmann and Neukum [14] chronology functions for Mars.

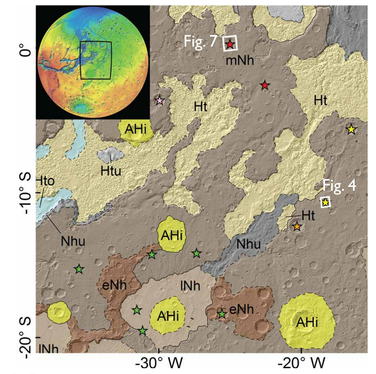

Fig. 2. Candidate sites (stars - yellow: Ubud-type, orange: possible Ubud-type, red: Type II, pink: possible Type II, green: uncertain type. Global geologic map [6] on MOLA hillshade [9].

3. Ubud-type ridges

Observations: Resistant regions of the existing substrate

Fracture-margin ridges with a broad, rounded morphology and composed of material consistent with the rest of the crater floor (Fig. 3) are seen in two impact craters in eastern Margaritifer.

They are best-imaged and most substantial in Ubud (Fig. 4), a 28 km-diameter impact crater south of Margaritifer chaos (-18.3°E, -10.6°N). Isolated outcrops of dark-toned capping material and morphological degradation of superposed impact craters indicate that the rugged crater floor has experienced erosion, and channels at the crater rim consistent with overspill suggest some erosion may have been accomplished by fluid upwelling from the fractures.

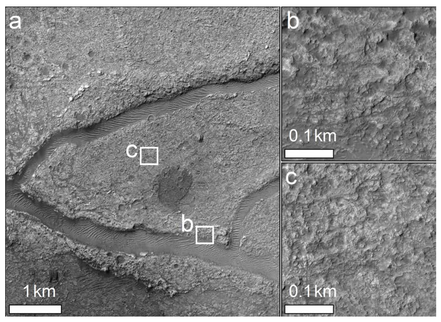

Fig. 3 (a) Fracture-margin ridges that have (b) the same light toned, brecciated morphology as (c) the surrounding substrate. (a) CTX B20_017317_1716, (b,c) HiRISE ESP_028354_1690.

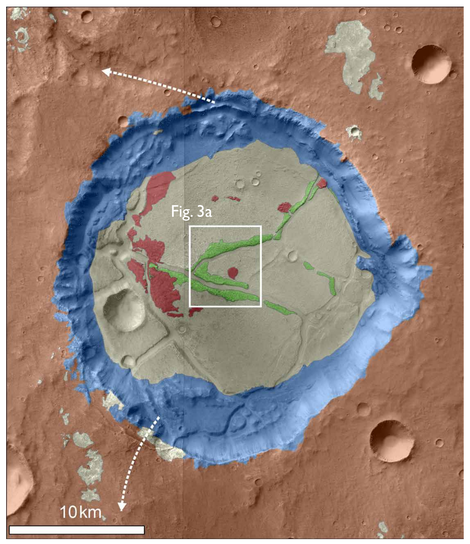

Fig. 4. Mapping shows ridges (green) along fractures in the rugged crater floor (yellow) of Ubud crater, which lies in Middle Noachian plains (brown). Dark-toned capping material (red) survives on the crater floor only locally, indicating erosional stripping. White dashed arrows indicate inferred directions of fluid overspill from the crater (base: CTX B20_017317_1716 and B18_016750_1715).

Interpretation: Subsurface mineral precipitation

The similarity of ridges to surrounding material and their rugged, rounded morphology indicate that they are erosion-resistant zones in crater floor material. Their occurrence along fractures suggests that they result from structurally-controlled subsurface induration by a mineral cement, as seen at Spencer Flat, Grand Staircase-Escalante, Utah. Here, iron (oxyhydr)oxide cementation occurred in the subsurface when oxidizing meteoric fluids channeled by joints met a reducing, Fe^{2+}-saturated subsurface reservoir [15]. The cemented zones now form ridges due to their superior resistance to erosion versus surrounding sandstones (Fig. 5).

Chemical precipitation can occur due to changes in pressure and temperature as well as by redox reactions; all of these factors would be expected to come into play as fluid rose from the deep, warm, reducing Martian subsurface to the oxidizing surface. Thus, subsurface precipitation at a geochemical boundary is a good explanation for cementation in Ubud's fracture wall-rock, as it is for cementation and chemical alteration along other structural lineaments on Mars [16,17].

Fig. 5. Iron (oxyhydr)oxide cement at a joint (right, Thomas for scale) renders a broad ridge of wall material resistant to erosion in Spencer Flat, Utah (left, Potter-McIntyre for scale).

4. Type II ridges

Observations: Steep-sided ridges overlying pre-existing substrate

Steeply-dipping ridges with flatter distal regions (Fig. 6) flank fractures in the floors of two unnamed craters in northern Margaritifer. The best imaged is 50 km south of Hydapsis Chaos (0.3°N, -25.1°E; Fig. 7). Though a lack of HiRISE imaging precludes determination of whether the texture of the ridge material differs from the surrounding crater floor, ridge material superposes pre-existing impact craters, indicating that the ridges considerably post-date floor formation and that they were emplaced at the surface.

There is evidence for both fracture-associated fluid flow (shallow channelization adjacent to fractures) and volcanism (a spectrally-distinct deposit around a northwest crater floor fracture) within this crater. Crater-count evidence suggests erosion by fluid and volcanism occurred contemporaneously.

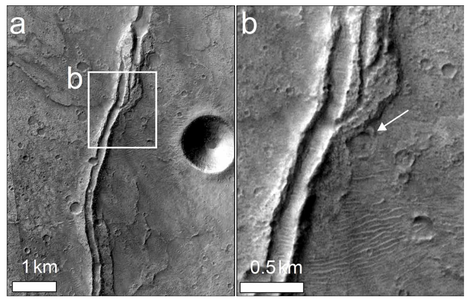

Fig. 6 (a) Ridges dip steeply away from the fracture, with flatter, broader distal regions. (b) Ridge material overlies a pre-existing 250 m diameter impact crater on the crater floor (CTX G19_025664_1803).

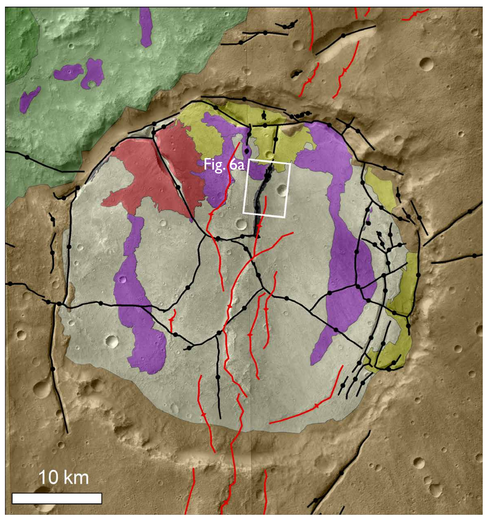

Fig. 7. Mapping of a crater south of Hydapsis chaos (green) shows an eroded crater floor (yellow) with capping units (purple) and a dark-toned deposit around a NW fracture. Ridges (black) run along central fractures. Surrounding plains (brown) overlie the crater's ejecta. Both the crater and plains are deformed by a series of wrinkle ridges (red lines), cross-cut by fractures (black lines) (base: CTX G22_026864_1798 and G19_025664_1803).

Interpretation: Subaerial deposition from fractures

The crater is not sufficiently closed to hold a crater lake and there is no evidence for one, so deposition is interpreted as subaerial. On Earth, subaerial ridge-like sedimentary deposits occur widely at spring sites:

- Hot springs: sulfurous [22] or siliceous [23,24,Fig. 8a] deposits, depending on the pH of upwelling fluid. On Mars, sulfur-enrichment would mostly occur only if circulating fluids directly took on dissolved volatiles from a degassing magmatic intrusion, but accumulation of dissolved silica would occur whenever hot fluids circulated through the basaltic crust [25].
- Cold springs: commonly travertine in fissure-ridge and terrace morphologies (Fig. 8b) similar to those seen at Type II Martian examples [18,19]. On Mars, an expected lack of subsurface carbonates renders carbonate cold spring precipitates improbable [20], but sulfates are a viable alternative [21].

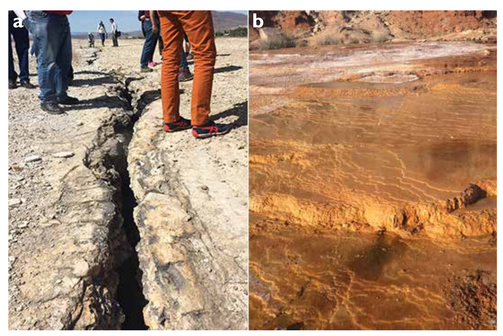

Fig. 8. Structurally-controlled surface deposition on Earth. (a) Siliceous sinter at a linear fissure, Steamboat (hot) Springs, Nevada. (b) Flat travertine terraces, Crystal Geyser cold spring, Utah; upwelling is controlled by Ten Mile Graben. Closest terrace face is ~10 cm high.

Neither spectral nor morphological data constrain which type of spring formed the Martian examples: there is no clear spectral anomaly at the ridges and both hot and cold spring deposits can have the observed morphology [23,26,27]. However, evidence for water flow and volcanic activity at the ridge sites and their occurrence in the most chaos-disrupted part of Margaritifer (attributed, according to many hypotheses, to the effects of subsurface magmatic intrusion), indicate a strong potential for a hydrothermal system here. Therefore, we propose that Type II ridges are mostly likely sulfurous or siliceous hydrothermal deposits, though further orbital and landed mineralogical data are required to verify this.

5. Conclusion: Good potential for astrobiological preservation

Chemical precipitates have the potential to encase any organisms living at the site of precipitation or entrained in the mineralizing fluid. Though conditions at the Martian surface in the Hesperian-Amazonian era of chaos and fracture-formation [6] are not expected to have been favorable to life, **potential habitability in the source regions of the upwelling fluid is good**. Even shallow groundwater on Mars comes from a zone that is shielded from inhospitable surface conditions, retains porosity and is minimally-altered [29]. Further, if fluids at Type II examples derived from a hydrothermal system, this will have been an especially warm, nutrient-rich source environment, potentially reaching to great depths if associated with a regional magmatic intrusion.

After mineral entombment, the potential for long-term preservation of biosignatures is good. Though syndepositional environmental fluctuations and diagenesis may have destroyed organic material [20,30], other biosignatures such as microbial fossils [23], biotically-mediated structures [31], and body molds [30] are found preserved in precipitates from both hot and cold settings on Earth. As silica is the most stable of the potential mineral precipitates mentioned here [25] and the best able to preserve biosignatures [32], **Type II ridges, if high-temperature siliceous precipitates, have the best biosignature preservation potential** of the two types.

References

[1] Wattel-Koekkoek E. J. W. et al. (2003) *Eur. J. Soil Sci.*, 54:2, 269–278.
[2] Farmer J.D. & Des Marais D.J. (1999) *J. Geophys. Res. Planets*, 104, 26977–26995.
[3] Malin M.C. et al. (2007) *J. Geophys. Res. Planets*, 112.
[4] McEwen A.S. et al. (2007) *J. Geophys. Res.*, 112.
[5] Malin, M. C. et al. (1992), *J. Geophys. Res.*, 97(E5), 7699–7718.
[6] Tanaka, K. L. et al. (2014), *Planet. Space Sci.*, 95, 11–24.
[7] Bamberg, M., R. et al. (2014), *Planet. Space Sci.*, 98, 146–162.
[8] Fergason, R. L., et al. (2006), *J. Geophys. Res. Planets*, 111(E12004).
[9] Smith, D. E. et al. (1999), *Science*, 284(5419), 1495–1503.
[10] Neukum, G., & R. Jaumann (2004), *ESA Spec. Publ.*, 1240, 17–35.
[11] Moratto, S. Z. et al. (2010), *Lunar Planet. Sci. Conf.*, 41, 2364.
[12] Christensen, P. R. et al. (2004), *Space Sci. Rev.*, 110, 85–130.
[13] Ivanov, B. A. (2001) in R. Kallenbach et al., Springer, 87–104.
[14] Hartmann, W. K., & G. Neukum (2001), *Space Sci. Rev.*, 96, 165–194.
[15] Potter, S. L., & M. A. Chan (2011), *Geofluids*, 11(2), 184–198.
[16] Okubo, C. H., & A. S. McEwen (2007), *Science*, 315(5814), 983–986.
[17] Treiman, A. H. (2008), *Nat. Geosci.*, 1(3), 181–183.
[18] De Filippis, L. et al. (2013), Earth-Science Rev., 123, 35–52.
[19] Brogi, A. et al. (2014), *J. Geol. Soc. London*, 171(3), 425–441.
[20] Chevrier, V. et al. (2007), *Nature*, 448(7149), 60–63.
[21] Rossi, A. P. et al. (2008), *J. Geophys. Res. Planets*, 113(8).
[22] Rodríguez, A. & M. J. van Bergen (2015), *Netherlands J. Geosci.*, 92(02), 153–169.
[23] Lynne, B. Y. et al. (2008), *Sediment. Geol.*, 210, 111–131.
[24] Campbell, K. A. et al. (2015), *Earth-Science Rev.*, 148, 44-64.
[25] Walter, M. R. & D. J. Des Marais (1993), *Icarus*, 101, 129–143.
[26] Brogi, A. & E. Capezzuoli (2009), *Int. J. Earth Sci.*, 98(4), 931–947.
[27] Sillitoe, R. H. (2015), *Miner. Depos.*, 50(7), 767–793.
[28] Frery, E. et al. (2015), *Tectonophysics*, 651, 121–137.
[29] Michalski, J. R. et al. (2013), *Nat. Geosci.*, 6(2), 133–138.
[30] Guidry, S. A. & H. S. Chafetz (2003), *J. Sediment. Res.*, 73(5), 806–823.
[31] Ruff, S. W. & J. D. Farmer (2016), *Nat. Commun.*, 7.
[32] Konhauser, K. O. et al. (2003), *Can. J. Earth Sci.*, 40(11).